Title: An altered cell type-specific subcellular distribu5on of translesion synthesis DNA polymerase kappa (PolK) in aging neurons

Authors: Mofida Abdelmageed, Shilpi Paul, and Anirban Paul[#].

Affiliation: Neural and Behavioral Sciences Department, Penn State College of Medicine, Hershey, PA 17033

Abstract

Genomic stability is critical for cellular function, however, postmitotic cells such as highly metabolically active neurons face the biggest challenge as they must maintain their genome over an organismal lifetime. DNA damage in neurons increases with chronological age and is accelerated in Alzheimer's disease, and neurodegenerative disorders, resulting in downstream cellular and systemic dysregulation. Distinct DNA damage response pathways have evolved with a host of distinct polymerases that act via different pathways such as nucleotide excision repair, and base excision repair to mend DNA lesions. The Y-family polymerases are known for their key role in bypassing damaged DNA through the process of translesion synthesis in dividing cells, however, their functions in enduring post-mitotic cell types like neurons are largely unknown. We show that one such member of the Y-family polymerases, DNA polymerase kappa protein (POLK), is subcellularly localized in the nucleus and cytoplasm of neurons. With chronological age, there is a significant reduction of nuclear POLK and a concomitant accumulation in the cytoplasm. The reduction of nuclear POLK in old brains is congruent with an increase in nuclear DNA damage. We further report that nuclear POLK expression is not uniform among cell types in the brain with significantly higher levels of nuclear POLK in GABAergic interneurons compared to excitatory pyramidal neurons and non-neurons, possibly reflective of the inherent biological differences such as axonal projection, neuronal activity, and their firing rates. Due to the non-replicative status of differentiated neurons in mature circuits, it is critical to understand the different repair strategies and mechanisms that postmitotic neurons employ to maintain their genomic integrity, which will help design therapies for human longevity and the prevention of neurodegeneration.

Title: An altered cell type-specific subcellular distribution of translesion synthesis DNA polymerase kappa (PolK) in aging neurons

Authors: Mofida Abdelmageed, Shilpi Paul, and Anirban Paul[#].

Affiliation: Neural and Behavioral Sciences Department, Penn State College of Medicine, Hershey, PA 17033

Introduction

Throughout the organismal lifespan, continuous exposure to exogenous and endogenous agents leads to damage to one or both strands of the DNA thus causing a persistent threat to genomic integrity [1–3]. Due to their long lifespan, increased transcriptional activity, and large energy demands, neurons are highly susceptible to cumulative DNA damage. Neuronal genomic enhancer regions are hotspots for constant high levels of DNA single-strand breaks (SSBs) repair synthesis process, thus revealing that neurons are undergoing localized and continuous DNA breakage [4]. In addition to genotoxins, the threat of genomic instability can also be contributed by normal 'programmed' DNA breaks like topoisomerase-induced breaks for the removal of topological stress during transcription. High levels of such 'programmed' DNA breakage occur in neurons, during neuronal development, differentiation, and maintenance [5]. A strong association exists between unrepaired DNA damage causing loss of genomic integrity with aging and neurodegeneration [3,4]. Hence survival strategies have evolved to preserve genomic stability

through multiple DNA damage response (DDR) pathways allowing the neurons to function effectively. Impaired DDR leads to genomic instability triggering signaling cascades [6] stalling transcription, and creating mutagenesis [7], thus altering the cellular fate toward anomalous cell cycle activation, apoptosis, or senescence, which are hallmarks of aging and age-associated diseases [8–11]. Indeed, mice defective in DNA repair synthesis polymerase(s) (Pol g and Pol b) show premature aging phenotype [12,13]. Neurons exhibit high levels of reactive oxygen species (ROS)-mediated DNA damage that generate SSBs by directly attacking the DNA backbone or by adding 8-oxo-7,8-dihydroguanine (8oxoG) modifications on DNA [14,15]. 8oxoG DNA lesions are often resolved through base excision repair (BER). Unrepaired SSBs hinder transcription and can also lead to DSBs. Due to the absence of cell cycling in the postmitotic neurons, the DSB repair is carried out only through the non-homologous end joining (NHEJ) and not by homologous recombination (HR).

One unique mechanism that bypasses DNA adducts, synthesize DNA past damage, and function in post-replication DNA repair such as NHEJ or BER is through translesion synthesis (TLS) DNA polymerases, and the Y-family DNA polymerases specialize in translesion synthesis [16,17]. TLS polymerases are well-studied in dividing cells, and there are four Y-family members Rev1, Pol kappa (Polk), Pol iota (Poli), and Pol eta (Polh). However, their role in post-mitotic cells is not explored. There is evidence of the role of Polk in dorsal root ganglion (DRG) neurons upon the treatment of genotoxic agents like cisplatin where Polk is upregulated [18], and is essential for efficiently and accurately repairing cisplatin crosslinks [19]. Polk can perform error-free TLS across bulky DNA adducts at N2 position of guanine induced by genotoxic agent benzo[a]pyrene-

dihydrodiol-epoxide (BPDE) and mitomycin C [20–22] . Polk can also bypass other DNA lesions including 8-oxo-guanine caused by oxidative stress[23–26]
in association with Werner syndrome helicase (WRN) protein [27] and through strand break repair mechanism [28] *Polk*$^{-/-}$ mice showed decreased survival compared to wild-type (WT) and heterozygous littermates, increased levels of spontaneous mutations and sensitivity to BPDE[29]. Separately, inactivated Polk knock-in mice showed a higher frequency of mutations, micronucleated cells, and DNA damage marker gH2AX foci compared to WT Polk. Furthermore, in *Polk*$^{-/-}$ mice high cholesterol diet promotes enhanced DNA mutagenesis and decreased survival in *apoE−/−;Polk−/−* [30]. Evidence supports that Polk can function in non-S phase cells through a NER-dependent mechanism to protect from UV-induced cytotoxic lesions [31,32]. Although Polk is associated with multiple DNA repair mechanisms, it remains unknown if normative age-associated DNA damage will also recruit Polk and how it may function in post-mitotic neurons.

Similar to neuronal DNA damage, other cells in the central nervous system are also susceptible to DNA damage, that leads to neurodegeneration. However, unlike the postmitotic neurons, the non-neuronal cells are able to go through the cell cycle and are replaceable utilizing the DNA repair process. Due to the non-replicative status of differentiated neurons in mature circuits, it is critical to understand the different repair strategies and mechanisms that postmitotic neurons employ to maintain their genomic integrity, which will help design therapies for human longevity and the prevention of neurodegeneration. Here we report the expression of POLK in the brain, its subcellular localization, how it is altered with chronological age, cell type-specific variability, and

the microglial engagement with neurons in wild-type mouse brains undergoing healthy aging under normative housing conditions.

Results:

A progressive age-associated shift in subcellular localization of Polk

First, we validated the anti-POLK antibody for immunofluorescence assays by knocking out Polk in the U2OS cell line [33] and recovering endogenous POLK by immunoprecipitation from cortical tissue. Comparative semiquantitative western blot of nuclear fractions from cortical tissue showed that POLK levels decreased with increasing age 1 month, versus 10 months and 18 months. To visualize this change at the subcellular level and perform a survey of POLK expression in the brain we developed an automated imaging pipeline that segments the nucleus and cytoplasm using the fluorescent Nissl that primarily stains cell bodies in brain sections [34] (Fig 1A-B). In the paraformaldehyde-fixed 60-micron brain tissue sections, POLK is detected as small speckles inside the nucleus at a young age (1-2 months) and larger granules can be seen in the cytoplasm at progressively older time points (>9 months). In young brains, both the normalized counts of nuclear POLK speckles and their size are consistent across the cingulate cortex (Cg1), motor cortex (M1 and M2), and somatosensory cortex (S1). A comparison of the nuclear POLK counts and size of speckles using ANOVA shows a significant age-associated decline with medium to large effect sizes across the four brain areas surveyed (Fig 1D-E and Tables 1 and 2) in agreement with the immunoblot assay. In the cytoplasm, on the other hand, there is a significant

age-associated accumulation of POLK in the form of increasingly larger-sized granules with decreasing total counts (Fig 1F, Tables 3 and 4)

Other TLS members follow a similar trend of decreased nuclear expression with age

To check if the age-associated decline in nuclear POLK is a more generalized phenomenon in Y-family TLS polymerases we tested Rev1 and Poli. REV1 protein is expressed as similar nuclear speckles it forms clusters of speckles in the nucleus. Like POLK, REV1 shows a qualitatively similar decline in nuclear expression and an increase in cytoplasmic granules in M1 and S1 brain areas at 1, 10, and 18 months. Comparatively, POLI nuclear expression was overall low with less impact at older ages (Fig 2) yet showed cytoplasmic accumulation.

Nuclear POLK co-localizes with DNA damage response and repair proteins in young brains

We conducted proteomics of the POLK complex from human cell lines[33] and tested if one of the identified DNA damage response proteins PRKDC can be observed in vivo. Upon co-immunostaining in 1-month-old brains, we observed that PRKDC expression was in the nucleus as distinct puncta that co-localizes with POLK puncta, which is lost in 10-month and 18-month-old brains (Fig 3).

POLK in the cytoplasm is associated with stress granules and lysosomes in old brains

To characterize the subcellular cytoplasmic localization of POLK in old brains, we co-immunostained with stress granule proteins G3BP1 and lysosomal protein LAMP1. In young 1-month brains, there was a minimal expression of G3BP1 and LAMP1 however by 18 months cytoplasmic POLK is almost entirely colocalized with both G3BP1 and LAMP1 in the cytoplasm indicating that older neurons are actively processing non-nuclear POLK for degradation.

Differentially altered POLK subcellular expression amongst excitatory, inhibitory, and non-neuronal cells in old brains.

To further test if the subcellular shift in POLK impacts all cells uniformly, we performed immunostaining to segregate excitatory, inhibitory, and non-neuronal cells in the brain. Old brain sections were co-immunostained with i) anti-NeuN to detect pan-neuronal protein RBFOX3, ii) anti-GAD67 to detect GABAergic neurons, iii) fluorescent Nissl to label all cells, and iv) anti-POLK to measure subcellular POLK levels. In a subset of samples, Gad67-Cre;Ai14 animals were also used to genetically label GABAergic neurons instead of anti-GAD67 immunostaining. Our original image quantitation pipeline was modified to register cells positive for GAD67, NeuN, and Nissl as GABAergic interneurons (IN), NeuN and Nissl positives as glutamatergic excitatory pyramidal neurons (PN), and Nissl positives only as non-neuronal (NN) cells (Fig 5 A-B). The INs and PNs were further segmented into their nuclear and cytoplasmic compartments whereas NN subcellular segmentation was not implemented due to the fact their nucleus occupies most of the cellular morphology[35]. Hence in NN, the POLK signal was considered to primarily represent the nuclear compartment. We restricted our survey to the GABAergic inhibitory and

glutamatergic excitatory neurons in cortical areas Cg1, M1, S1, and RSD which have no dopaminergic, serotonergic, cholinergic, glycinergic, and histaminergic neuronal cell bodies. Brain samples were derived from healthy animals monitored by trained veterinary staff, maintained under a constant 12hrs light-dark cycle in a barrier facility on standard mouse chow, never subjected to any pharmacological treatment or stressful behavioral tests, and ranged between 18-24 months of age at the time of harvesting brain tissue. Strikingly, in the old brains across the four cortical areas observed, the nuclear POLK signal was consistently highest in the cell group identified as INs, followed by PNs and NNs. ANOVA shows that these differences are highly significant with large effect sizes (Fig 5C). In contrast, the cytoplasmic POLK signal was not significantly different between IN and PNs in the old brains (Fig 5D).

Microglia associated IN and PN have significantly lower levels of nuclear POLK and higher levels of cytoplasmic POLK.

Microglia cells in the brain are known to remove synapses and cell bodies and overactive microglia have been associated with neurological disorders. To test any relationship of INs and PNs with microglia, we surveyed by immunostaining old brains with microglia marker protein IBA1. 20x images were analyzed to register IBA1, Nissl positive cells as microglia (MG) and GAD67, NeuN, and Nissl positive cells as IN and NeuN and Nissl positive cells as PN. IN or PNs where MG cells are overlapping or directly in contact are scored as MG-tied IN or MG-tied PN, those that are within one MG cell body length proximity are scored as MG-adjacent IN or MG-adjacent PN, and IN and PN cell bodies that are removed by more than one MG cell body length from an IN and PN

are scored MG-free IN and PN (Fig 6 A-B). We then compared the nuclear and cytoplasmic POLK counts between the MG-tied IN and MG-free INs as well as MG-tied and MG-free PNs. Strikingly MG-tied INs and PNs have significantly more cytoplasmic POLK compared to MG-free INs and PNs with a large effect size (Fig 6C). However, there were minimal differences in nuclear POLK counts between MG-tied and MG-free INs and PNs (Fig 6D).

Discussion

An endogenous "aging clock" for brain tissue

There have been multiple approaches towards estimating biological age using "aging clocks" using sequencing, from tissue and body fluids using epigenetic marks [36] and multi-omics approach [37]. Further genomic instability is increasingly associated with neuronal activity and aging, with Progeroid syndromes are often linked to genomic instability [38]. So we hypothesized that it may be possible to use protein expression of polymerases such as POLK to determine the biological age of tissue sections. Hence, we tested if the subcellular localization of POLK can be a learnable feature that can predict organismal age. We split 75% of the data and trained a classifier on the POLK nuclear and cytoplasmic counts among other parameters and validated on 25% hold-out group to test if organismal age is discernible and found that it is indeed possible to predict 1-month, 10-month, and 18-month age brains with ROC values >0.8 (Fig 7A). Cytoplasmic and nuclear POLK counts combined comprised ~70% drove the classifier relative influence. Using a similar strategy, we note that in old brains nuclear POLK counts alone drive ~90% of the difference

in distinguishing IN, PN, and NN with ROC > 0.8 (Fig 7B), suggesting cell groups IN, PN, and NN have an inherent biological relationship in how they utilize TLS polymerase POLK in old age.

Our study provides primary evidence that cell classes experience aging pressure differentially and as recent studies progressively provide a clearer picture of the cell-type diversity in the brain it remains to be investigated which subsets are the more innately resilient and vulnerable under normative aging, and how genotoxic and pathological conditions can act as a modifier.

Figure legends:

Figure 1: Polk subcellular expression changes with increasing age, across multiple cortical regions.

A) Schematic of animals used in this aging study.

B) Visualization of Polk speckles (green) expression using immunohistochemistry in cells labeled by fluorescent-nissl (red) from wild-type mouse brain aged 1 month, and 18 months.

C-D) Representative low (20x) and high magnification (63x) images showing the subcellular distribution of Polk as speckles (arrowheads) in the nucleus and larger granules in the cytoplasm (arrows) in brain areas Cg1, M1, M2, and S1. D. For each corresponding brain areas raincloud, boxplots and density plots show the nuclear Polk counts decreasing with increasing age. ANOVA values are shown in table 01.

E) Means plots with 95% confidence intervals showing the nuclear Polk speckle count and size decreasing with increasing age in Cg1, M1, M2, and S1 cortical areas.

F) E) Means plots with 95% confidence intervals show the cytoplasmic Polk granule count decreasing with a concomitant increase in size with age in Cg1, M1, M2, and S1 cortical areas. Cells counted are the total number evaluated for each age group.

Figure 2: TLS polymerases Rev1 and PolI subcellular expression also change in the mouse brain with increasing age.

A) Visualization of Rev1 protein expression (green) using immunostaining in cells counterstained with fluorescent-nissl (purple) from M1 and S1 cortical regions in ages 1 month, 10 months, and 18 months.

B) Visualization of Poli protein expression (green) using immunostaining in cells counterstained with fluorescent-nissl (purple) from M1 and S1 cortical regions in ages 1 month, 10 months, and 18 months.

Arrowheads point nuclear speckles and arrows indicate cytoplasmic granules.

Figure 3. Colocalization of PolK with DNA damage marker proteins

A) Sparse nuclear expression of DNApkC/Prkdc co-localizes with Polk nuclear speckles in young 1M old brain.

B) Gamma H2AX co-localizes with Polk nuclear speckles in 12 M old brain.

Figure 4: Cytoplasmic Polk expression co-localizing with stress granules and lysosomal proteins

A) Cytoplasmic Polk (green) expression co-localizing with G3BP1 (blue) in fluorescent-nissl stained cells (purple) of mouse brain tissue from M1 and S1 cortical regions in 18 months old brain but not in young 1 month.

B) Cytoplasmic Polk (green) expression co-localizing with LAMP1 (blue) in fluorescent-nissl stained cells (purple) of mouse brain tissue from M1 and S1 cortical regions of 18-month brain.

Figure 5: Nuclear Polk is differentially expressed based on cell-type in old brains.

A) Representative image of the detection of inhibitory interneurons (IN), excitatory pyramidal neurons (PN) and non-neuronal (NN) cell bodies using automated image analysis pipeline from a four-channel image of cortical areas.

B) Magnified view of the dotted box from subpanel A showing overlay of the nuclear, cytoplasmic segmentation outlines and detection of nuclear Polk speckles and cytoplasmic Polk granules in IN, PN and NN cells from Cg1, M1, S1, and RSD cortical regions in wild type mice brain.

C) Boxplots from brain areas show the nuclear Polk count is higher in INs than PNs and NNs.

D Boxplots from brain areas show the cytoplasmic Polk count is not significantly different between INs than PNs.

Figure 6: Microglia associated with INs and PNs show significantly higher levels of cytoplasmic Polk expression.

A) A representative single 20x imaging field shows outlines of detected cell bodies of IN (red), PN (green). Iba1+ microglia (MG) that are attached or wrapped to neurons (MG-tied, filled light pink and arrows) and microglia that are within one body length of a neuron (blue fill with an asterisk) as well as unassociated microglia (blue fill).

B) Shows separation of the four-channel super-resolution confocal image, fluorescent-nissl, NeuN, and Gad67 = IN, fluorescent-nissl, and NeuN = PN, and fluorescent-nissl, and Iba1 = MG.

C) Minimal difference in nuclear Polk speckle counts between subsets of MG free and MG tied among the IN and PN populations. The subset of the MG free IN and PN show a slight increase in nuclear Polk counts compared to MG tied population.

D) Significant and large effect size difference in cytoplasmic Polk granule counts between subsets of MG free and MG tied among the IN and PN populations.

Figure 7: Subcellular expression of Polk is a learnable feature predictive of organismal age in wild-type mice brain tissue and broad cell class at old age.

A) Boosting classification can distinguish between 1-month, 10-month, and 18-month-old images upon training on the subcellular nuclear and cytoplasmic distribution of Polk counts and validating on holdout samples. Receiver Operator Curve (ROC) values show the performance of the classifier for each age group when tested on the holdout groups. The bar plot shows the relative contribution of the image parameters and metadata, where cytoplasmic and nuclear Polk together account for ~70% relative influence on the classifier performance.

B) Nuclear Polk count drives ~90% of classifier performance in distinguishing IN, PN, and NN in old (>18 months) age brains suggesting Polk levels may reflect the distinctly differential metabolic and biological demands between these broad cell classes.

Methods

Experimental Animals

STRAIN:010802
IMSR_JA:010802

Immunohistochemistry Assay

To detect Polk presence in the brain, we conducted a series of IHC experiments in 1-month (young), 10- months (middle age) and 18-months (old) mice brains. For brain tissue extraction, animals were anesthetized with ketamine (conc?). Animals were then perfused using 1x phosphate buffered saline (PBS) and 4% paraformaldehyde (PFA). Tissue were fixed with 4% PFA overnight, and stored in 10% sodium azide. The fixed tissue was sectioned at 60µm thickness using a vibratome. For the IHC protocol, tissue underwent a blocking step consisting of donkey serum, 1x PBS, and 10% Triton X-100 at RT for 2 hours. Tissue were washed 3x with PBS at RT for10 minutes. For visualization of Polk in the brain, we used a monoclonal primary mouse anti-Polk IgG1k antibody at a 1:200 dilution along with a secondary IgG donkey anti-mouse antibody containing a fluorophore of 488 at 1:1000 dilution (protocol 1). We immuno-stained all cells using fluorescent Nissl 647 at 1:300 dilution for 20 minutes at RT to distinguish the sub-cellular compartments Polk is localized.

For detection of Poli and Rev1, we followed a similar IHC procedure, however our optimization worked best with goat-serum. We visualized Rev1 using a mouse monoclonal IgG1 k Rev1 antibody at a 1:400 dilution along with a secondary goat anti-mouse 488 antibody at 1:1000. We also used fluorescent Nissl 647 at 1:300 dilution to stain all cells. We detected Poli using a mouse monoclonal IgG3 k DNA Poli antibody at 1:400 dilution with a secondary IgG3 goat anti-mouse 594 at 1:1000. To avoid spillover on the fluorescent channels, we used fluorescent Nissl 435 at 1:300.

To determine whether Polk and DNA-PKCs are colocalized, we conducted a co-staining experiment in young and old mice brains. In our initial Polk staining we used donkey serum; in this experiment we used goat serum which worked similar as our previous optimization for Polk (1:200). We used a secondary goat anti-mouse 488 antibody at 1:1000 (protocol 2). For detecting DNA-PKCs, we used a rabbit anti-DNA PKCs at a 1:500 dilution with a secondary goat anti-rabbit 594 at 1:1000. We used Nissl 647 at 1:300 to stain all cells.
We conducted an experiment to test whether cytoplasmic Polk if colocalizes with stress granules. We stained for stress granules and Polk in young and old brains. For visualization of the stress granules, we used the primary monoclonal IgG2a mouse anti-G3BP1 antibody at a dilution of 1:18 with a secondary goat anti mouse 594 antibody at 1:1000 dilution. Since G3BP1 and the Polk antibodies shared the same host, for this Polk staining we used a secondary IgG1 goat anti-mouse 488 antibody (protocol 3). Due to the IgG1 antibody being more sensitive for detecting Polk, we re-optimized the Polk protocol and concluded using a 1:400 dilution for the primary antibody and 1:2000 dilution for the secondary antibody. We used Nissl 647 at 1:300 to stain all cells.
We then conducted a second series of experiments using the old mice brains to determine if there is a relationship between cytoplasmic Polk and lysosomes localization. We used the same Polk

optimization from the G3BP1 experiment to detect Polk. For detecting lysosomes, we used a monoclonal rat anti Lamp1 IgG2a antibody with a 1:500 dilution and a goat anti rat 594 secondary antibody. We used Nissl 647 at 1:300 to stain all cells.

To investigate if there is more microglia activation localized near cytoplasmic Polk accumulation. We stained for Polk using the same concentration and antibodies from the stress granules and lysosomes experiments. For visualization of microglia, we used a rabbit anti-Iba1 primary antibody with a 1:1000 dilution and a goat anti rabbit 594 secondary antibody at 1:250 dilution. We used Nissl 435 to stain all cell bodies.
To determine if there is a cell-type difference of the distribution of Polk subcellularly.

Confocal Microscopy, Image Analysis, Quantification, and Statistical Analysis

Imaging was performed by super resolution confocal microscopy using Zeiss LSM910 with AiryScan2 in multiplex mode SR-2Y using 40X water and 63X oil objectives. The imaging parameters such as laser power, digital gain, digital offset, scan speed was kept the same for all samples in each experiment.
Images were quantified through a tailored-made pipeline through CellProfiler (CITE). Images were split based on imaging channels for objects detection. In all images the Nissl channel was used to identify the nucleus and cytoplasm of each cell. Polk speckle count and size were detected in all nuclei and cytoplasm.

References

1. Hou Y, Song H, Croteau DL, Akbari M, Bohr VA. Genome instability in Alzheimer disease. Mech Ageing Dev. 2017 Jan 1;161:83–94.

2. Yan S, Vaziri C. An introduction for the special issue on environmental health and genome integrity. Environ Mol Mutagen. 2020;61(7):660–663.

3. Welch G, Tsai L. Mechanisms of DNA damage-mediated neurotoxicity in neurodegenerative disease. EMBO Rep. 2022 May 2;23(6):e54217. PMCID: PMC9171412

4. Wu W, Hill SE, Nathan WJ, Paiano J, Callen E, Wang D, Shinoda K, van Wietmarschen N, Colón-Mercado JM, Zong D, De Pace R, Shih HY, Coon S, Parsadanian M, Pavani R, Hanzlikova H, Park S, Jung SK, McHugh PJ, Canela A, Chen C, Casellas R, Caldecott KW, Ward ME, Nussenzweig A. Neuronal enhancers are hotspots for DNA single-strand break repair. Nature. Nature Publishing Group; 2021 May;593(7859):440–444.

5. Caldecott KW, Ward ME, Nussenzweig A. The threat of programmed DNA damage to neuronal genome integrity and plasticity. Nat Genet. Nature Publishing Group; 2022 Feb;54(2):115–120.

6. Fagagna F d'Adda di, Reaper PM, Clay-Farrace L, Fiegler H, Carr P, von Zglinicki T, Saretzki G, Carter NP, Jackson SP. A DNA damage checkpoint response in telomere-initiated senescence. Nature. Nature Publishing Group; 2003 Nov;426(6963):194–198.

7. Vermeij WP, Dollé MET, Reiling E, Jaarsma D, Payan-Gomez C, Bombardieri CR, Wu H, Roks AJM, Botter SM, van der Eerden BC, Youssef SA, Kuiper RV, Nagarajah B, van Oostrom CT, Brandt RMC, Barnhoorn S, Imholz S, Pennings JLA, de Bruin A, Gyenis Á, Pothof J, Vijg J, van Steeg H, Hoeijmakers JHJ. Restricted diet delays accelerated ageing and genomic stress in DNA-repair-deficient mice. Nature. Nature Publishing Group; 2016 Sep;537(7620):427–431.

8. Yousefzadeh M, Henpita C, Vyas R, Soto-Palma C, Robbins P, Niedernhofer L. DNA damage—how and why we age? Simon M, Tyler JK, editors. eLife. eLife Sciences Publications, Ltd; 2021 Jan 29;10:e62852.

9. Rutten BPF, Schmitz C, Gerlach OHH, Oyen HM, de Mesquita EB, Steinbusch HWM, Korr H. The aging brain: Accumulation of DNA damage or neuron loss? Neurobiol Aging. 2007 Jan 1;28(1):91–98.

10. Petr MA, Tulika T, Carmona-Marin LM, Scheibye-Knudsen M. Protecting the Aging Genome. Trends Cell Biol. Elsevier; 2020 Feb 1;30(2):117–132. PMID: 31917080

11. McKinnon PJ. Genome integrity and disease prevention in the nervous system. Genes Dev. 2017 Jun 15;31(12):1180–1194.

12. Trifunovic A, Wredenberg A, Falkenberg M, Spelbrink JN, Rovio AT, Bruder CE, Bohlooly-Y M, Gidlöf S, Oldfors A, Wibom R, Törnell J, Jacobs HT, Larsson NG. Premature ageing in mice expressing defective mitochondrial DNA polymerase. Nature. Nature Publishing Group; 2004 May;429(6990):417–423.

13. Kujoth GC, Hiona A, Pugh TD, Someya S, Panzer K, Wohlgemuth SE, Hofer T, Seo AY, Sullivan R, Jobling WA, Morrow JD, Van Remmen H, Sedivy JM, Yamasoba T, Tanokura M, Weindruch R, Leeuwenburgh C, Prolla TA. Mitochondrial DNA mutations, oxidative stress, and apoptosis in mammalian aging. Science. 2005 Jul 15;309(5733):481–484. PMID: 16020738

14. Nakamura J, Swenberg JA. Endogenous apurinic/apyrimidinic sites in genomic DNA of mammalian tissues. Cancer Res. 1999 Jun 1;59(11):2522–2526. PMID: 10363965

15. Attwell D, Laughlin SB. An energy budget for signaling in the grey matter of the brain. J Cereb Blood Flow Metab Off J Int Soc Cereb Blood Flow Metab. 2001 Oct;21(10):1133–1145. PMID: 11598490

16. Sale JE, Lehmann AR, Woodgate R. Y-family DNA polymerases and their role in tolerance of cellular DNA damage. Nat Rev Mol Cell Biol. Nature Publishing Group; 2012 Mar;13(3):141–152.

17. Gao Y, Mutter-Rottmayer E, Zlatanou A, Vaziri C, Yang Y. Mechanisms of Post-Replication DNA Repair. Genes. Multidisciplinary Digital Publishing Institute; 2017 Feb;8(2):64.

18. Zhuo M, Gorgun MF, Englander EW. Translesion Synthesis DNA Polymerase Kappa Is Indispensable for DNA Repair Synthesis in Cisplatin Exposed Dorsal Root Ganglion Neurons. Mol Neurobiol. 2018 Mar 1;55(3):2506–2515.

19. Jha V, Ling H. Structural Basis for Human DNA Polymerase Kappa to Bypass Cisplatin Intrastrand Cross-Link (Pt-GG) Lesion as an Efficient and Accurate Extender. J Mol Biol. 2018 May 25;430(11):1577–1589.

20. Kanemaru Y, Suzuki T, Sassa A, Matsumoto K, Adachi N, Honma M, Numazawa S, Nohmi T. DNA polymerase kappa protects human cells against MMC-induced genotoxicity through error-free translesion DNA synthesis. Genes Environ. 2017 Jan 7;39:6. PMCID: PMC5219776

21. Ogi T, Shinkai Y, Tanaka K, Ohmori H. Polkappa protects mammalian cells against the lethal and mutagenic effects of benzo[a]pyrene. Proc Natl Acad Sci U S A. 2002 Nov 26;99(24):15548–15553. PMCID: PMC137754

22. Avkin S, Goldsmith M, Velasco-Miguel S, Geacintov N, Friedberg EC, Livneh Z. Quantitative analysis of translesion DNA synthesis across a benzo[a]pyrene-guanine adduct in mammalian cells: the role of DNA polymerase kappa. J Biol Chem. 2004 Dec 17;279(51):53298–53305. PMID: 15475561

23. Zhang Y, Yuan F, Wu X, Wang M, Rechkoblit O, Taylor JS, Geacintov NE, Wang Z. Error-free and error-prone lesion bypass by human DNA polymerase kappa in vitro. Nucleic Acids Res. 2000 Nov 1;28(21):4138–4146. PMCID: PMC113145

24. Haracska L, Prakash L, Prakash S. Role of human DNA polymerase kappa as an extender in translesion synthesis. Proc Natl Acad Sci U S A. 2002 Dec 10;99(25):16000–16005. PMCID: PMC138554

25. Jałoszyński P, Ohashi E, Ohmori H, Nishimura S. Error-prone and inefficient replication across 8-hydroxyguanine (8-oxoguanine) in human and mouse ras gene fragments by DNA polymerase kappa. Genes Cells Devoted Mol Cell Mech. 2005 Jun;10(6):543–550. PMID: 15938713

26. Kamiya H, Kurokawa M. Mutagenic bypass of 8-oxo-7,8-dihydroguanine (8-hydroxyguanine) by DNA polymerase κ in human cells. Chem Res Toxicol. 2012 Aug 20;25(8):1771–1776. PMID: 22804710

27. Maddukuri L, Ketkar A, Eddy S, Zafar MK, Eoff RL. The Werner syndrome protein limits the error-prone 8-oxo-dG lesion bypass activity of human DNA polymerase kappa. Nucleic Acids Res. 2014 Oct 29;42(19):12027–12040.

28. Zhang X, Lv L, Chen Q, Yuan F, Zhang T, Yang Y, Zhang H, Wang Y, Jia Y, Qian L, Chen B, Zhang Y, Friedberg EC, Tang TS, Guo C. Mouse DNA polymerase kappa has a functional role in the repair of DNA strand breaks. DNA Repair. 2013 May 1;12(5):377–388.

29. Stancel JNK, McDaniel LD, Velasco S, Richardson J, Guo C, Friedberg EC. Polk mutant mice have a spontaneous mutator phenotype. DNA Repair. 2009 Dec 3;8(12):1355–1362.

30. Singer WD, Osimiri LC, Friedberg EC. Increased dietary cholesterol promotes enhanced mutagenesis in DNA polymerase kappa-deficient mice. DNA Repair. 2013 Oct 1;12(10):817–823.

31. Ogi T, Lehmann AR. The Y-family DNA polymerase κ (pol κ) functions in mammalian nucleotide-excision repair. Nat Cell Biol. Nature Publishing Group; 2006 Jun;8(6):640–642.

32. Sertic S, Mollica A, Campus I, Roma S, Tumini E, Aguilera A, Muzi-Falconi M. Coordinated Activity of Y Family TLS Polymerases and EXO1 Protects Non-S Phase Cells from UV-Induced Cytotoxic Lesions. Mol Cell. 2018 Apr 5;70(1):34-47.e4. PMID: 29551515

33. Paul S, Rebok A, Cifani P, Paul A, Pappin D, Huang TT, Spratt TE. Translesion DNA synthesis polymerase kappa functions in the nucleolar stress response [Internet]. bioRxiv; 2022 [cited 2023 Sep 27]. p. 2022.10.27.513845. Available from: https://www.biorxiv.org/content/10.1101/2022.10.27.513845v1

34. Paul CA, Beltz B, Berger-Sweeney J. The Nissl Stain: A Stain for Cell Bodies in Brain Sections. Cold Spring Harb Protoc. Cold Spring Harbor Laboratory Press; 2008 Sep 1;2008(9):pdb.prot4805. PMID: 21356903

35. García-Cabezas MÁ, John YJ, Barbas H, Zikopoulos B. Distinction of Neurons, Glia and Endothelial Cells in the Cerebral Cortex: An Algorithm Based on Cytological Features. Front Neuroanat [Internet]. 2016 [cited 2022 Oct 5];10. Available from: https://www.frontiersin.org/articles/10.3389/fnana.2016.00107

36. Grodstein F, Lemos B, Yu L, Iatrou A, De Jager PL, Bennett DA. Characteristics of Epigenetic Clocks Across Blood and Brain Tissue in Older Women and Men. Front Neurosci [Internet]. 2021 [cited 2022 Feb 19];14. Available from: https://www.frontiersin.org/article/10.3389/fnins.2020.555307

37. Nie C, Li Y, Li R, Yan Y, Zhang D, Li T, Li Z, Sun Y, Zhen H, Ding J, Wan Z, Gong J, Shi Y, Huang Z, Wu Y, Cai K, Zong Y, Wang Z, Wang R, Jian M, Jin X, Wang J, Yang H, Han JDJ, Zhang X, Franceschi C, Kennedy BK, Xu X. Distinct biological ages of organs and systems identified from a multi-omics study. Cell Rep. 2022 Mar 8;38(10):110459. PMID: 35263580

38. Gurkar AU, Niedernhofer LJ. Comparison of mice with accelerated aging caused by distinct mechanisms. Exp Gerontol. 2015 Aug 1;68:43–50.

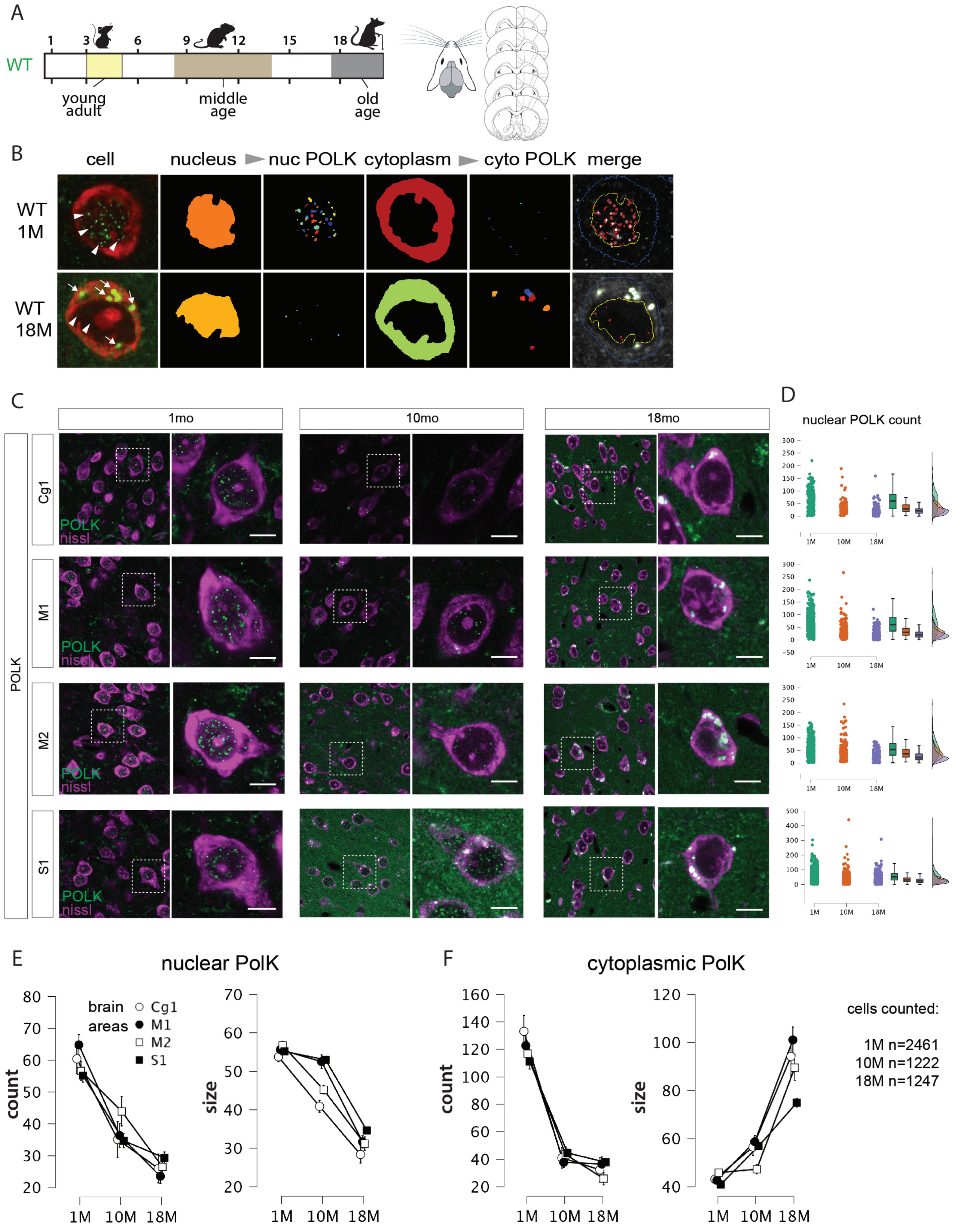
A
WT
1
3
6
9
12
15
18
young adult
middle age
old age
B
cell
nucleus
nuc POLK
cytoplasm
cyto POLK
merge
WT 1M
WT 18M
C
1mo
10mo
18mo
POLK
nissl
Cg1
M1
M2
S1
D
nuclear POLK count
1M
10M
18M
E
nuclear PolK
brain areas
Cg1
M1
M2
S1
count
size
F
cytoplasmic PolK
count
size
cells counted:
1M n=2461
10M n=1222
18M n=1247

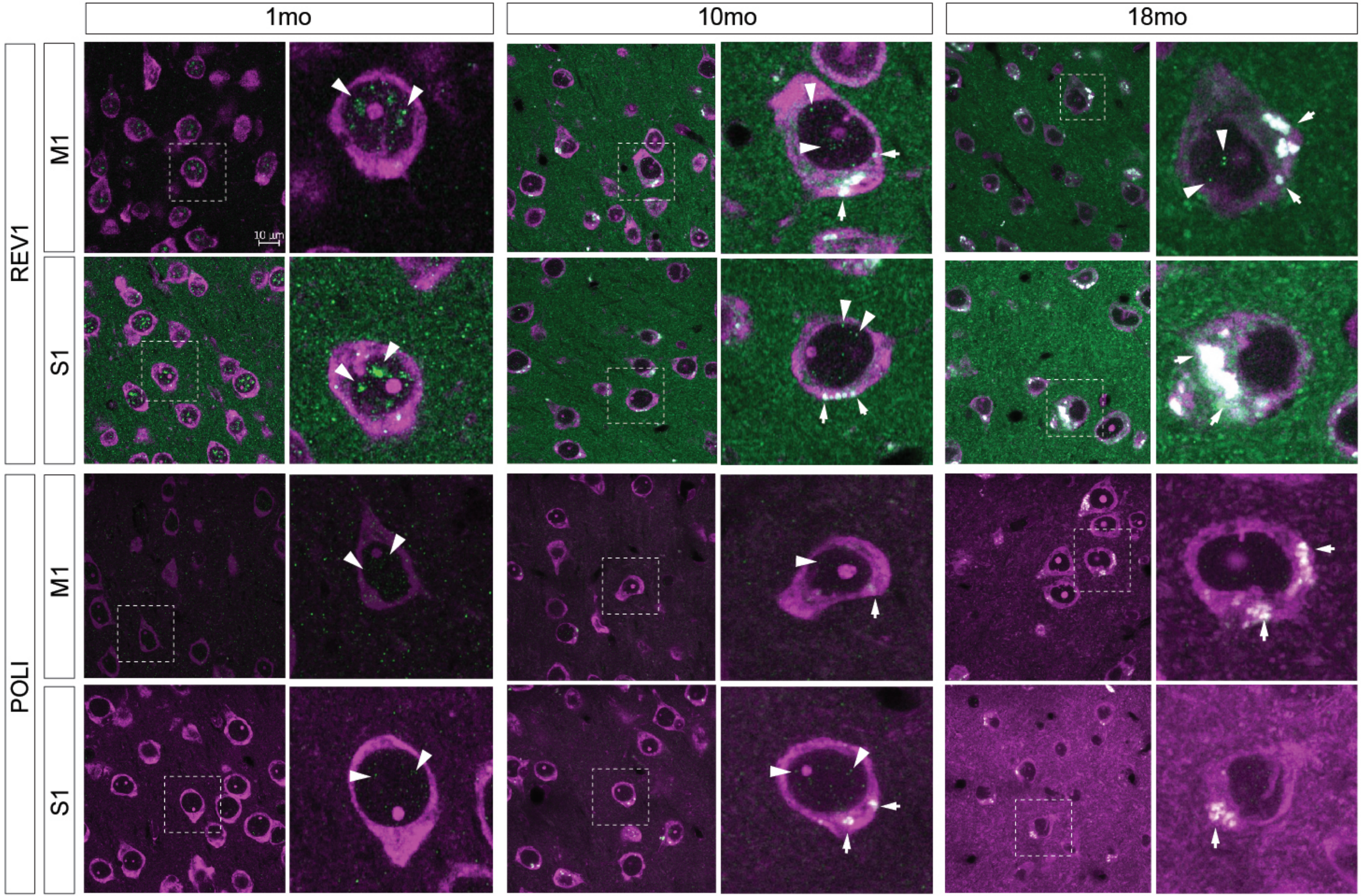
1mo
10mo
18mo
REV1
POLI
M1
S1
M1
S1
10 µm

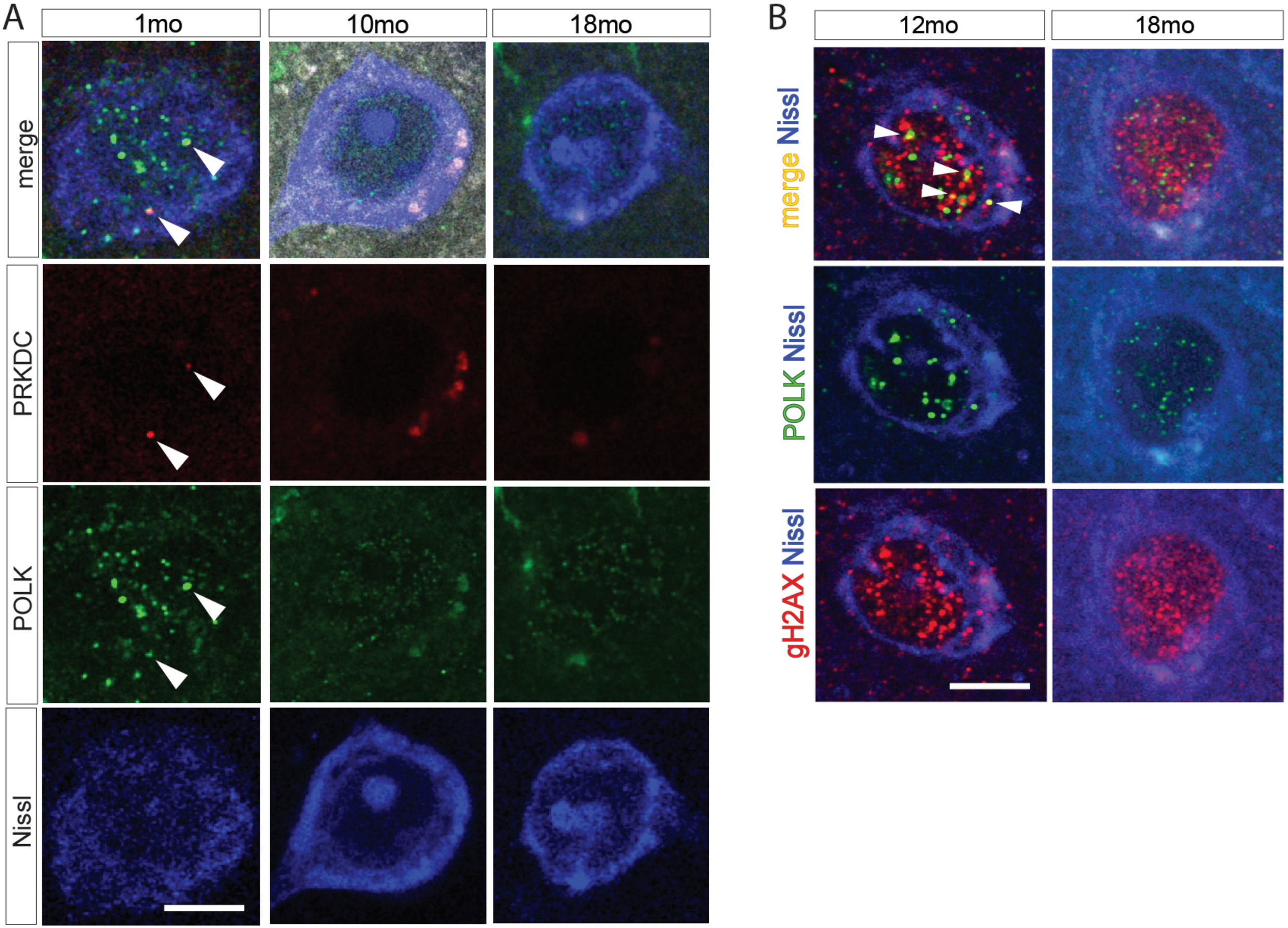
A
1mo
10mo
18mo
merge
PRKDC
POLK
Nissl
B
12mo
18mo
merge Nissl
POLK Nissl
gH2AX Nissl

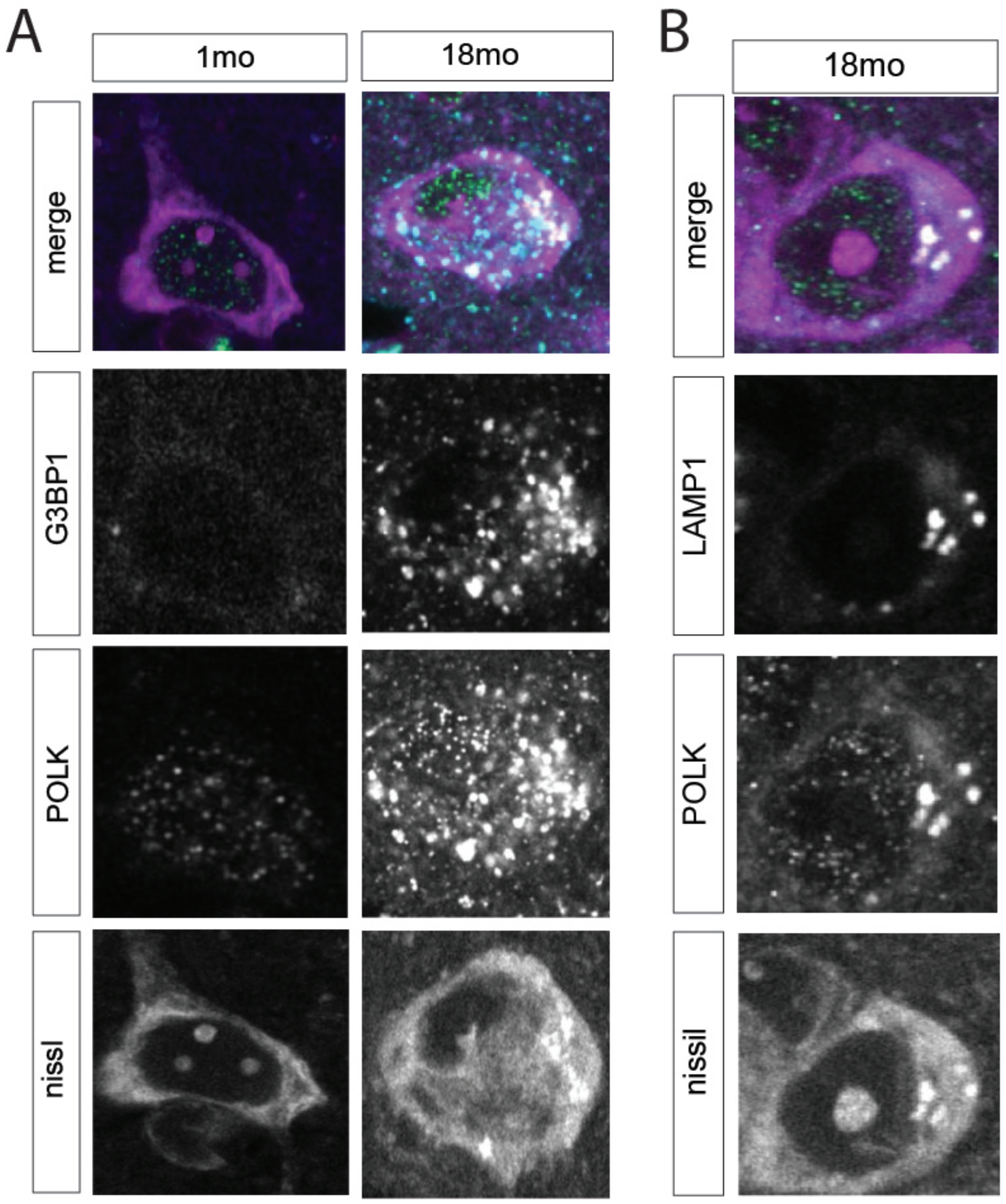
A
1mo
18mo
merge
G3BP1
POLK
nissl
B
18mo
merge
LAMP1
POLK
nissil

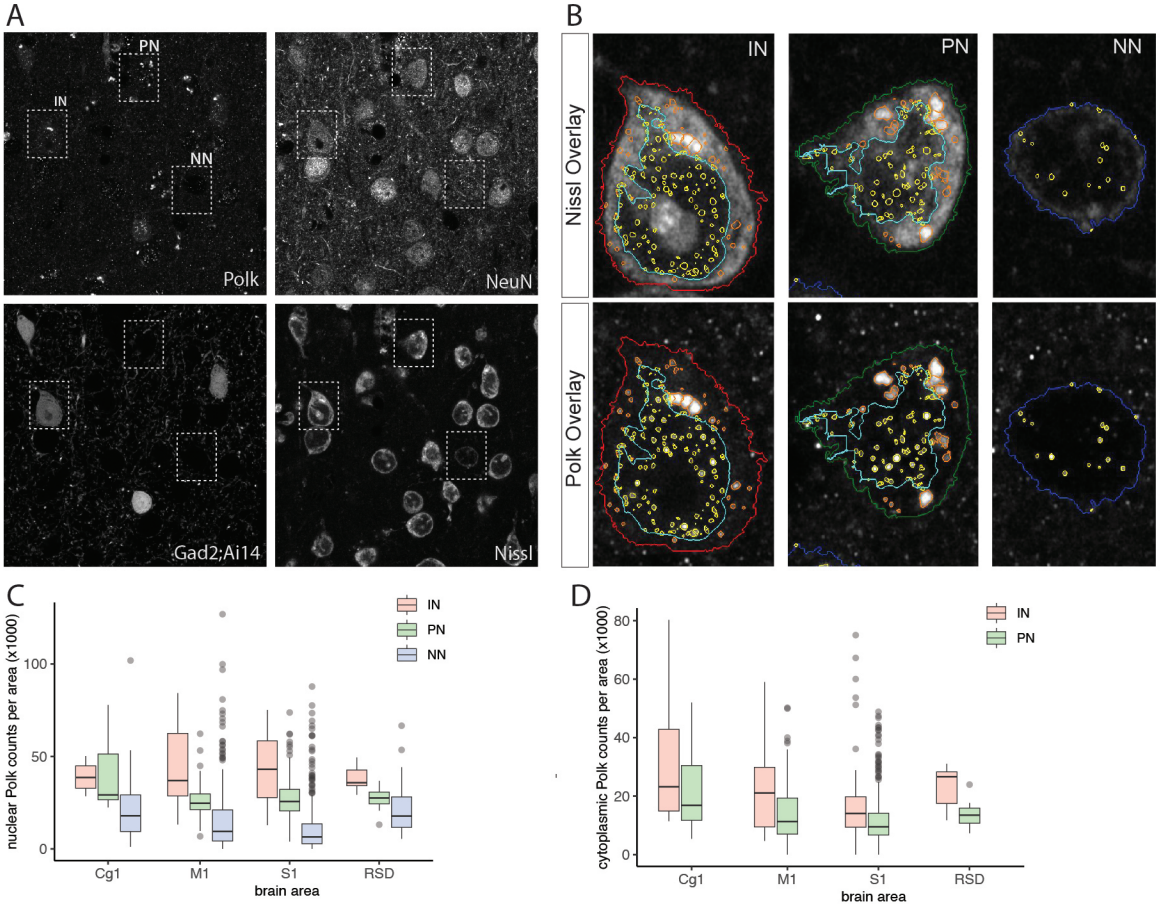
A
PN
IN
NN
Polk
NeuN
Gad2;Ai14
Nissl
B
Nissl Overlay
Polk Overlay
IN
PN
NN
C
nuclear Polk counts per area (x1000)
0
50
100
IN
PN
NN
Cg1
M1
S1
RSD
brain area
D
cytoplasmic Polk counts per area (x1000)
0
20
40
60
80
IN
PN
Cg1
M1
S1
RSD
brain area

A

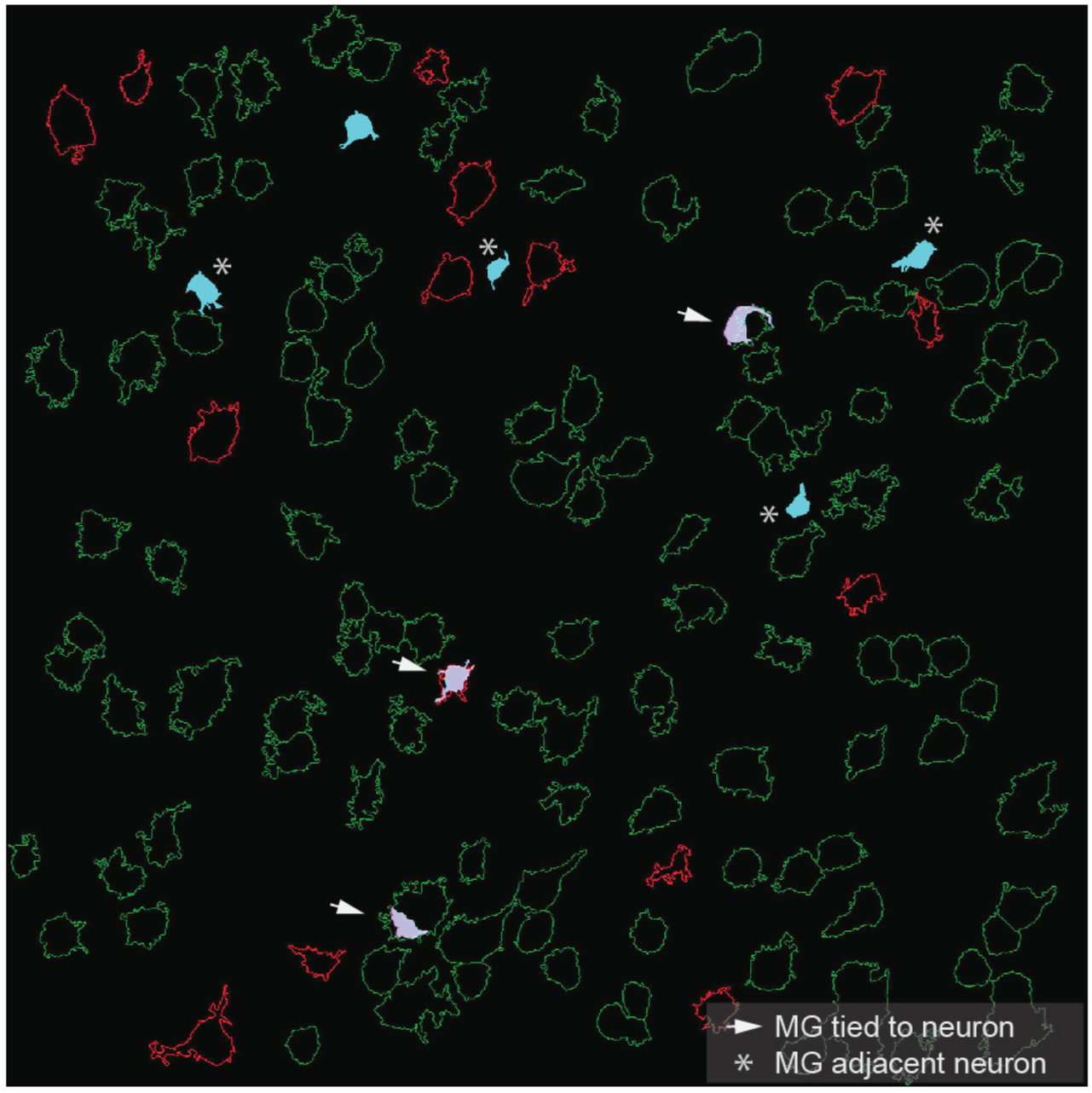
MG tied to neuron
MG adjacent neuron

B

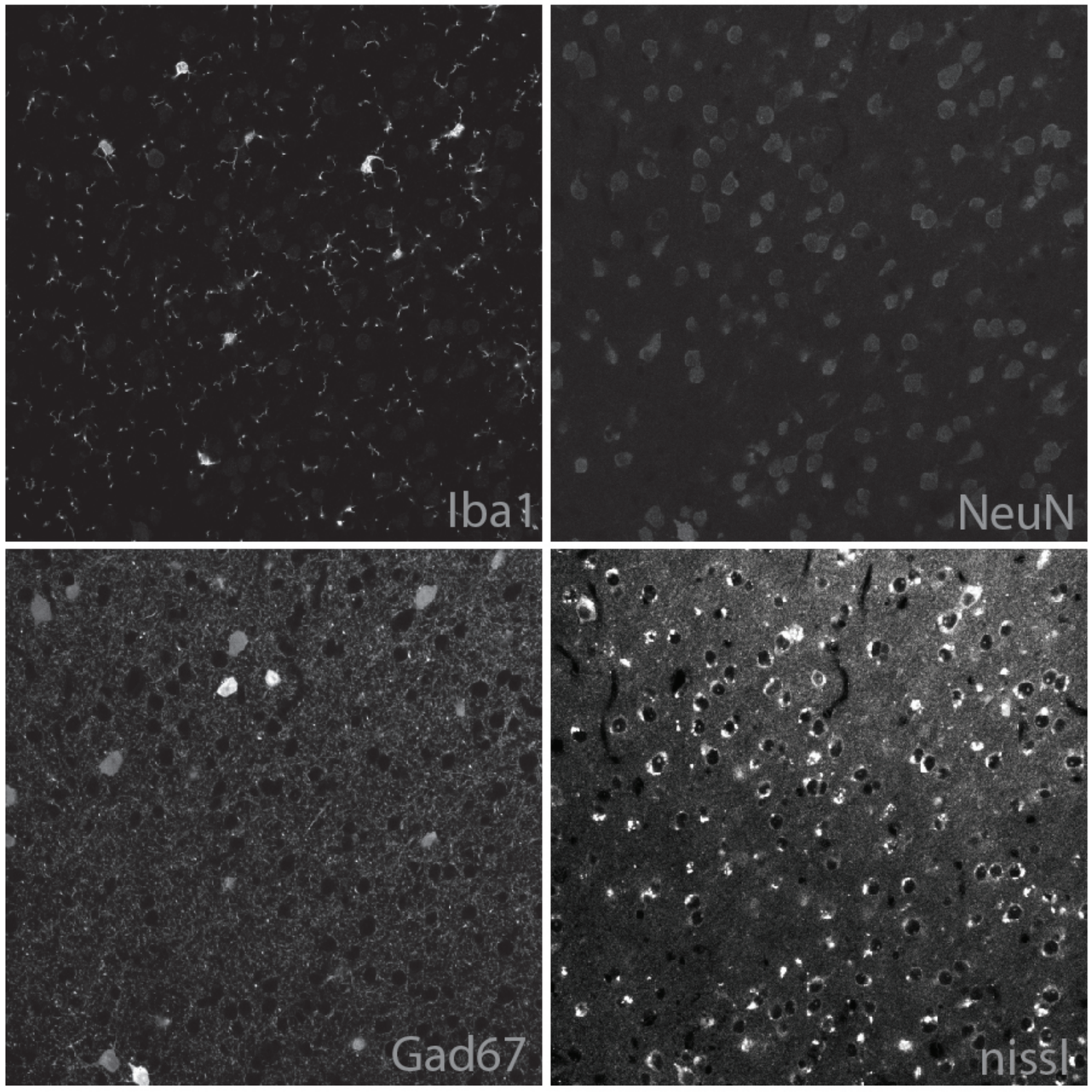
Iba1
NeuN
Gad67
nissl

C

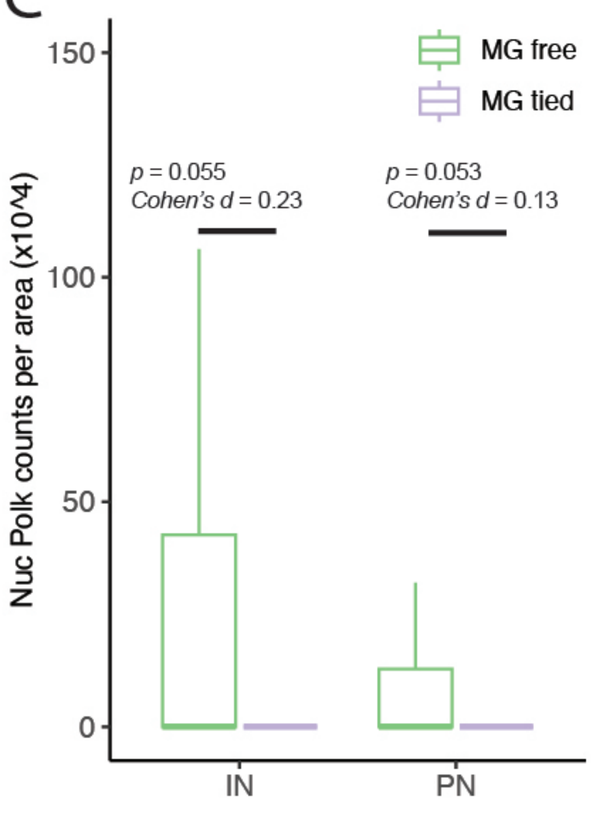
MG free
MG tied
p = 0.055
Cohen's d = 0.23
p = 0.053
Cohen's d = 0.13
Nuc Polk counts per area (x10^4)
150
100
50
0
IN
PN

D

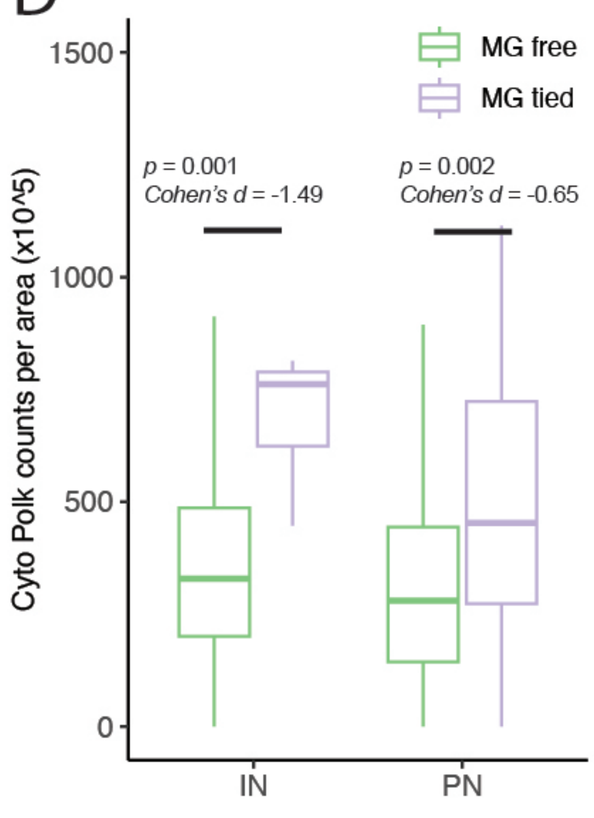
MG free
MG tied
p = 0.001
Cohen's d = -1.49
p = 0.002
Cohen's d = -0.65
Cyto Polk counts per area (x10^5)
1500
1000
500
0
IN
PN

A

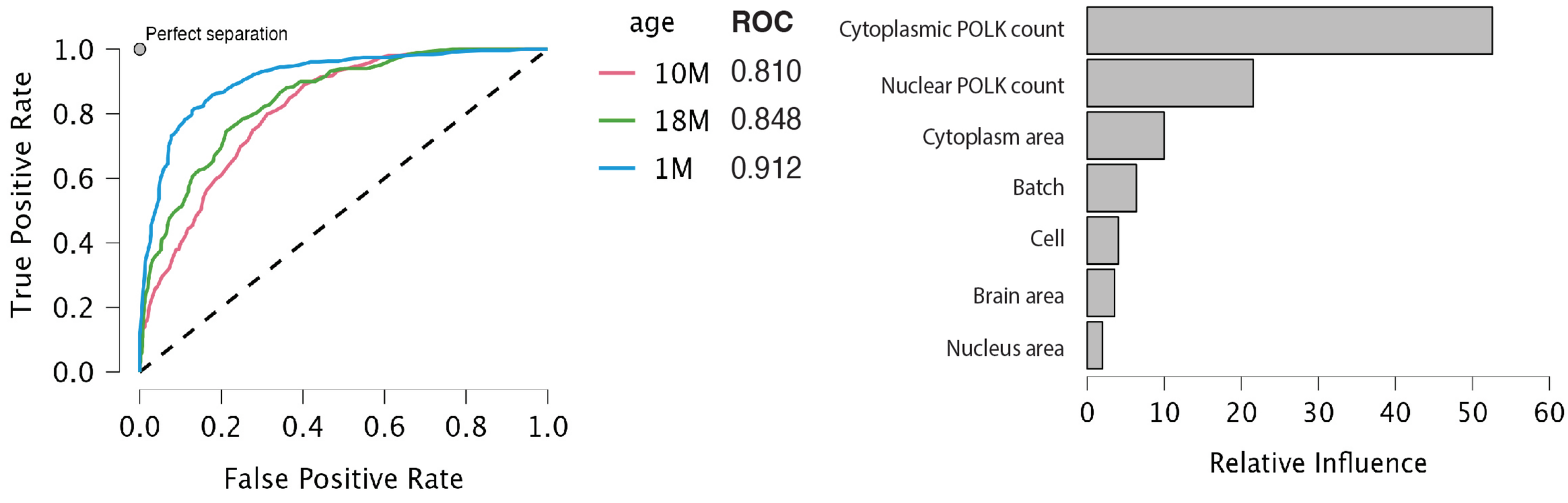
Perfect separation
True Positive Rate
False Positive Rate
0.0
0.2
0.4
0.6
0.8
1.0
age
ROC
10M 0.810
18M 0.848
1M 0.912
Cytoplasmic POLK count
Nuclear POLK count
Cytoplasm area
Batch
Cell
Brain area
Nucleus area
0
10
20
30
40
50
60
Relative Influence

B

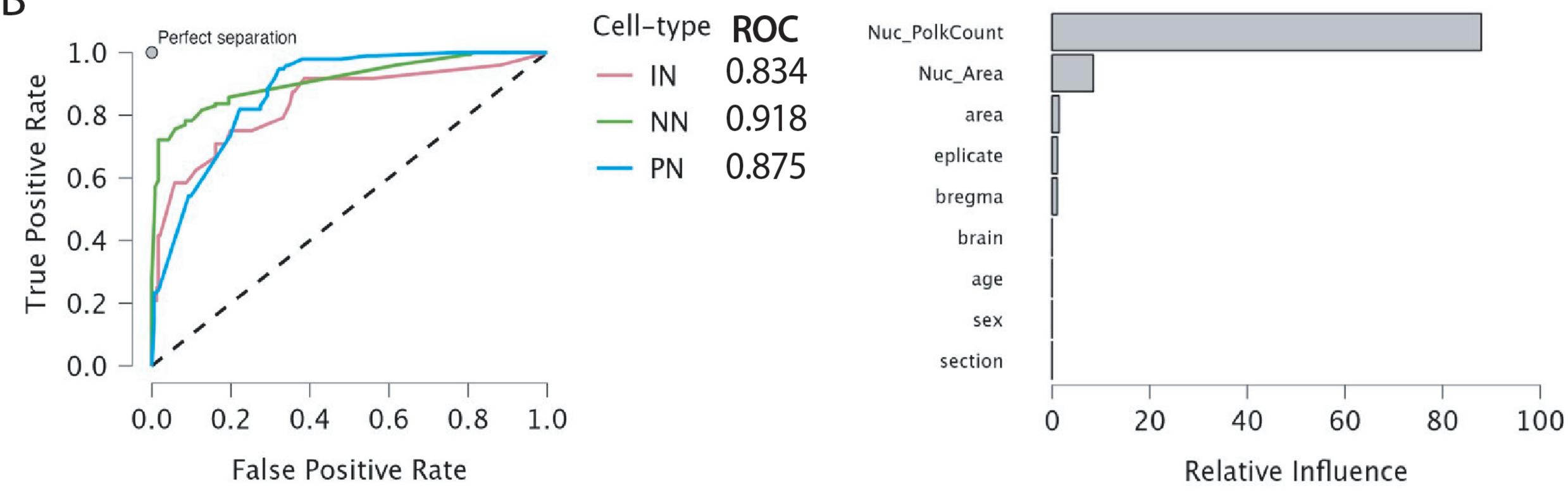
Perfect separation
True Positive Rate
False Positive Rate
0.0
0.2
0.4
0.6
0.8
1.0
Cell-type
ROC
IN 0.834
NN 0.918
PN 0.875
Nuc_PolkCount
Nuc_Area
area
eplicate
bregma
brain
age
sex
section
0
20
40
60
80
100
Relative Influence